JMEPEG (2010) 19:347–355
DOI: 10.1007/s11665-009-9496-5

1059-9495/$19.00

Influence of Surface Preparation on the Kinetics of Controlled Gas-Nitrided AISI H13 Steels Used in Extrusion Dies

S.S. Akhtar, A.F.M. Arif, B.S. Yilbas, and A.K. Sheikh

(Submitted November 15, 2008; in revised form March 25, 2009)

In the aluminum extrusion practice, gas nitriding represents an important factor in enhancing the service life of AISI H13 steel dies. It is observed that if the die-bearing surface is not adequately prepared before nitriding, a nonuniform and shallow nitrided layer develops with reduced hardening effect. The focus of this paper is to investigate the influence of different surface conditions in terms of roughness on the kinetics of nitrided layer developed during gas-nitriding process under controlled nitriding potential. Four samples made of AISI H13 steel properly heat treated (quenched and tempered) were considered: without surface preparation, ground, polished, and lapped. All the samples were gas nitrided under the same conditions and examined after being nitrided. The nitrided layers were characterized using different techniques including optical microscopy, scanning electron microscopy, x-ray diffraction analysis, energy dispersive spectrometry mapping, and microhardness analysis. It was found that the surface preparation prior to nitriding significantly enhanced the nitriding kinetics, which in turn resulted in even and deep nitrided case depth. This provided high load-bearing capacity due to increased and deep hardening effect as compared to unprepared sample. A thinner and uniform compound layer with well-resolved phases was achieved in comparison with unprepared sample.

Keywords AISI H13 steel, gas nitriding, metallurgical analysis, surface preparation

1. Introduction

Aluminum extrusion die is susceptible to considerable frictional forces at the die-bearing surface due to heat generation and high pressure in the extrusion process. The hard oxide film, which forms instantly on the surface of the extruded aluminum, causes extensive wear of the die bearing during service. Improvement in wear resistance is one of the big challenges for the extruders as gas nitriding is a very sensitive process about achieving and maintaining consistent and quality nitrided structure. Apart from other aspects, preparation of die-bearing surface before nitriding is a common practice followed in aluminum extrusion industry using different surface activation operations like polishing, etc. The surface activation is usually considered as positive treatment in terms of wear resistance by enhancing the quality and properties of nitrided layer, resulting in better die performance.

Gas nitriding involves atomic nitrogen from dissociating ammonia gas at temperatures in the range 450-590 °C diffusing into the steel surface. The nitriding of the steel can be visualized by bringing N_2 into contact with the surface of workpiece under extremely high pressure, which becomes possible by using NH_3 mixed with either N_2 or H_2 (Ref 1-3). Formation of the nitrided case begins with a series of nucleated growth areas on the surface of the steel. The near-surface microstructure of nitrided alloy steels consists of a compound zone which is made up of mainly iron nitrides. These nitrides occur as epsilon phase (ε-$Fe_{2-3}N$), gamma phase (γ′-Fe_4N), or mixed phase. Below the compound layer, the diffusion zone is formed which is composed of stable nitrides comprising substitution alloying elements and interstitial nitrogen. The area below the diffusion zone is the core of the steel consisting of tempered martensite. For tool steels, strong nitride-forming elements in diffusion zone include: Cr, V, Mo, and W. Cr is the major nitride-forming element in H13 steel which contributes to about 5% in the composition. The hardening effect in the diffusion zone is due to the presence of these nitride-forming elements which are finely dispersed pinning dislocations. The hardness of the nitrided surface may exceed 1000 HV (Ref 4).

Sueyoshi et al. (Ref 5) examined the influence of the mechanical pretreatment on gas-nitriding behavior of austenitic stainless steels and found that nitriding reaction can be enhanced markedly with increasing surface roughness when its value exceeds 6 and 1 μm for SUS310 and SUS316 steels, respectively, whereas no reaction is observed for the surface roughness less than these values. Czelusniak et al. (Ref 6) showed that soft and shallow nitrided case is achieved in H13 steel extrusion dies if the bearing surface of the die is not activated before gas nitriding. They suggested that bearing surface of die should be properly polished for effective nitriding. Bei et al. (Ref 7) studied the effects of surface ultrasonic peening (SUSSP) on gas nitriding of mild steel. They observed that when gas nitriding below 560 °C, SUSSP treatment could not only enhance both diffusion coefficient and mass transfer coefficient dramatically during gaseous

S.S. Akhtar, A.F.M. Arif, B.S. Yilbas, and **A.K. Sheikh**, Department of Mechanical Engineering, King Fahd University of Petroleum & Minerals, Box 1913, Dhahran 31261, Saudi Arabia. Contact e-mail: bsyilbas@kfupm.edu.sa.

nitriding process but also reduces the threshold nitriding potential. With this surface treatment before gas nitriding, the nitriding rate can be accelerated so dramatically that nitriding time can be reduced to half, or the conventional nitriding temperature could reduce approximately 50%. Wroblewski and Skalski (Ref 8) demonstrated that the combination of shot peening with gas nitriding on Armco iron leads to a change in surface layer formation as well as to the improvement in its properties. The plastic deformation generated by the glass shot impacts stimulates diffusion processes and results in increased thickness of nitrided layer in comparison with classical gas nitriding. Baranowska et al. (Ref 9) investigated that cathode sputtering used as a pretreatment before gas nitriding increases the rate of nitride layer formation in iron. They reported that ground sample exhibits thicker nitrided layer after nitriding as compared to polished sample due to the structural changes observed in the ground samples. They considered surface activation as a positive effect on the gas-nitriding kinetics.

In this paper, the effect of prenitriding surface preparation of AISI H13 steel on the behavior of gas-nitriding process under controlled nitriding potential is studied with the aim to find how efficiently surface activation can be used for better die performance. The nitrided layers of three samples, which were ground, polished, and lapped before nitriding, were studied in terms of morphology of diffusion zone and compound layer, case depth, and hardness-depth profile. Sample without surface preparation (designated as unprepared sample) is also included in the investigation for comparison purpose. All the samples were properly heat treated (quenched and tempered) prior to surface preparation and subjected to the same nitriding cycle.

2. Experimental Procedures

2.1 Sample Preparation

Rectangular samples ($10 \times 10 \times 4$ mm^3) of H13 tool steel (ORVAR 2 Microdized) were used in the experiments. A typical die steel used for hot extrusion dies have the following composition (in wt.%): 0.39 C, 1 Si, 0.4 Mn, 5.3 Cr, 1.9 Mo, 0.9 V, and balance Fe. The samples were heat treated with proper environmental control using vacuum furnace to prevent decarburization. The heat treatment cycle included: stress relieving at 650 °C, preheating at 815 °C, austenitizing at 1030 °C, quenching, and finally double tempering (first at 550 °C and second at 605 °C). After first tempering, the expected embrittling effects of coarse carbide structure, formed by the transformation of retained austenite to tempered martensite, were alleviated by subsequent second tempering step.

The samples were prepared with three different surface finishing conditions: (a) Ground samples, which were prepared with 320-grit abrasive paper; (b) Polished samples, which were prepared with polishing cloth using successive steps from 3 to 0.25 μm water-based diamond suspension; and (c) Lapped samples, which were prepared on a lapping machine with a wheel rotation of 500 rpm. The surface roughness (R_a) values were measured using a surface roughness tester.

2.2 Nitriding Cycle Used for Samples

A nitriding technology with state-of-the-art equipment and a user-friendly software program, allowing full automation of all functions, process stages, and safety procedures with closed-loop processing parameters, was used in collaboration with local industrial setup. The system was capable of maintaining the preset values of nitriding potential ($K_n = p_{NH_3}/(p_{H_2})^{3/2}$, where p is the partial pressure of constituting gas). The values of nitriding potentials (K_n) were maintained within certain limits as desired for each processing stage by continuous self-correction. The system set the flows for nitrogen and ammonia according to the preset program. Figure 1(a) shows the variations of temperature and gas flow rate (Q, L/min) in the retort during two-stage nitriding. Operating parameters were: Stage 1—490 °C and set-point K_n: 6.4 $(atm)^{-1/2}$ and Stage 2—530 °C and set-point K_n: 0.323 $(atm)^{-1/2}$. The furnace was first preheated and equalized to the preset temperature (450 °C) for about 3 h. The air in the retort was replaced by the ammonia and nitrogen gas mixture. The filling time (1 h and 40 min) was calculated automatically by the control system, based on the furnace volume and incoming gas flow. During each process stage, the temperature and gas flow were controlled to achieve the set-point K_n values, which depends upon ammonia dissociation percentage. The variation of K_n during the nitriding cycle is shown in Fig. 1(b) and was recorded at an interval of 10 min; in which case, K_n variation depicted the decrease of ammonia percentage from stage 1 to stage 2 (i.e., an atmosphere with increased dissociation of ammonia from stage 1 to stage 2). The heat stages were activated automatically before the next process stage commenced. The time of heating 1 and heating 2 prior to stage 1 and stage 2, respectively, was set to 1 h. The process time for stages 1 and 2 were 1.5 and 3.3 h, respectively. After the second stage, a cooling fan was automatically activated until the preset cooled temperature (110 °C) level was achieved. The total nitriding cycle took about 15 h; however, the actual nitriding time was about 6.8 h corresponding to heating 1 through stage 2 as illustrated in Fig. 1(a). Based on the recommended ranges, K_n values for different stages as classified by aerospace material specification (AMS) (Ref 10) in accordance with the requirement of AMS 2759/10A was adopted.

2.3 Nitrided Layer Characterization

Samples were polished and lapped using OMNILAP 2000 lapping machine (South Bay Technology Inc., CA, USA). Surface roughness of the samples was measured by SJ-400 Surface Roughness Tester (Mitutoyo Corporation, Tokyo, Japan). The samples were cut into two pieces after nitriding and cross-sectioned for optical and scanning electron microscopy. The cross sections were investigated using Axioplan 2 imaging optical microscope (Gottingen, Germany). The samples were first mounted, and the cross sections were polished with diamond paste (initially with 3 μm and finally with 0.25 μm) and etched with nital (1 vol% HNO_3 in ethyl alcohol) for about 7 s before examination. The specimens were cleaned ultrasonically prior to etching. The SEM micrographs were analyzed with Jeol JSM-6460LV scanning electron microscope (Tokyo, Japan) equipped with energy dispersive spectrometry (EDS). EDS mapping techniques was used for qualitative analysis of nitrided layer microstructure. X-ray diffraction analysis (XRD) was used for the determination of phase characterization of nitrided surfaces using LabX XRD-6000 x-ray diffractometer (SHIMADZU, Kyoto, Japan). Measurements were made using Cu-Kα radiations in the scan range $2\theta = 10°$-$80°$ with a step size of 0.02°. International Centre for Diffraction Data (ICDD) database was used for the identification of phases from the

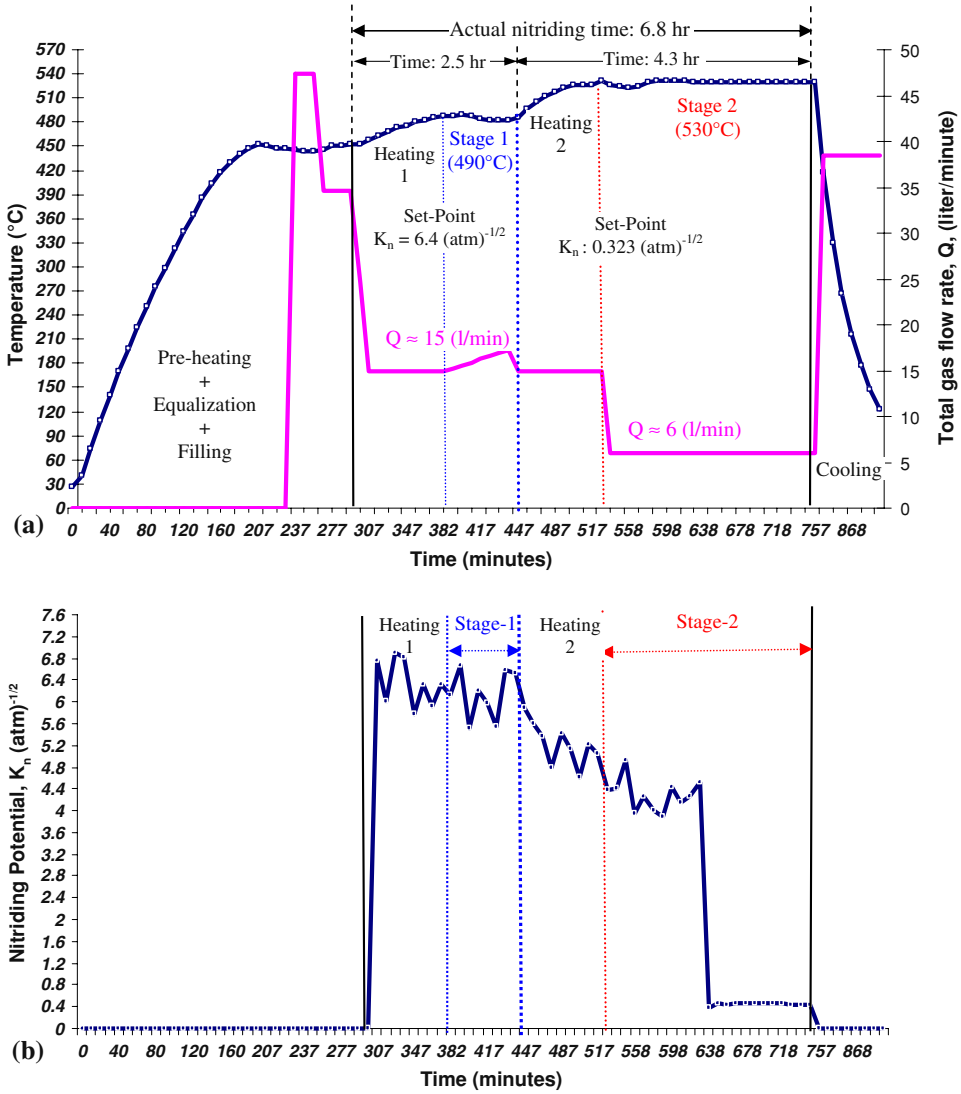

Fig. 1 Variations of temperature and flow rate of gas mixture, NH_3 and N_2 (a) and nitriding potential (K_n) (b) into the retort during two-stage nitriding of AISI H13 samples

positions of diffraction peaks. The microhardness measurements were performed across the cross sections of the nitrided specimens using BUEHLER Wirtz Vickers test apparatus (Dusseldorf, Germany) under an applied load of 100 g.

3. Results and Discussion

3.1 XRD Measurement and Phase Analysis

Figure 2 shows the XRD diffractograms for the surface of unprepared, ground, polished, and lapped samples after gas-nitriding treatment. The major phases in the surface of all samples are iron nitrides, which confirm the presence of the superficial compound layer. The major phases identified in the unprepared sample are ε-Fe_3N corresponding to (110) and (200) planes with a small peaks of mixed nitride phases' peak of ε-Fe_3N (002) + γ′-Fe_4N (111) and ε-Fe_3N (112). Moreover, additional ε-Fe_3N peaks were also observed corresponding to (101), (103), and (113) planes for surface-treated samples. A small peak of ε-Fe_3N (110) was also observed in ground and polished sample. The various iron nitride peaks indicate that surface preparation facilitates the incorporation of more nitrogen atoms into the subsurface diffusion zone. High-intensity peak of α-Fe (110) + CrN (200) in the case of surface-treated samples were observed which can be associated with a thin compound layer. Since the compound layer is thin, it is probable that the Fe and CrN reflections were detected from the subsurface diffusion matrix and not due to the compound layer. No pronounced ferrite (α-Fe) and CrN peaks were detected in the as-received sample. This is because of the compound layer thickness which is larger than the x-ray penetration depth, as the Cu-K_α probes to few microns. The values of lattice spacing (d) corresponding to α-Fe (110) is shown in Table 1. The d-values reduce with increasing prenitriding surface roughness (R_a). These reduced d-values with increasing R_a are also associated with corresponding increase in 2θ values. The reduced lattice spacing in ground sample having highest initial surface roughness of (0.13 ± 0.035) μm after gas nitriding can be associated with the highest compressive stress. The high compressive stress is likely due to comparatively more number

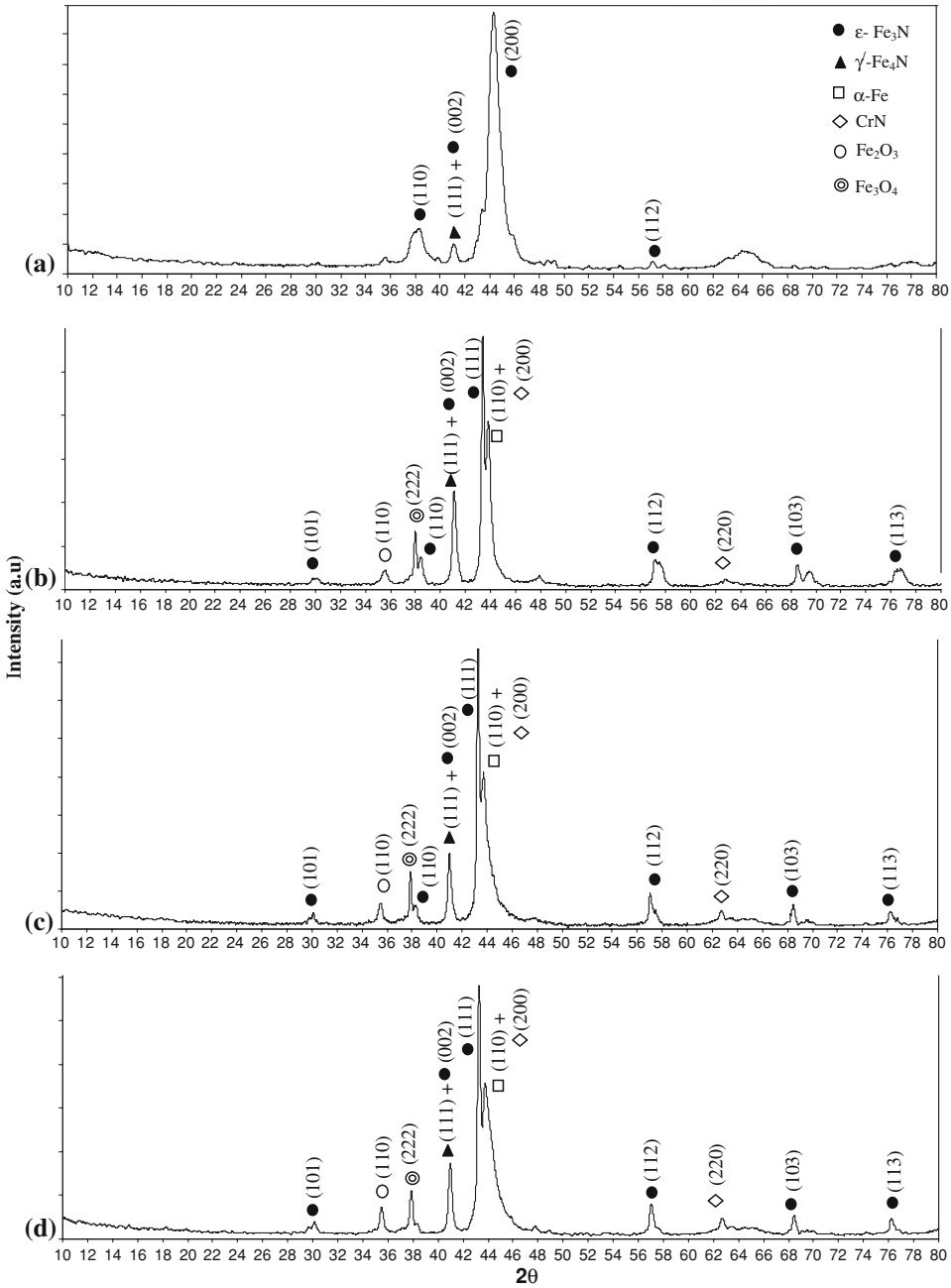

Fig. 2 XRD diffractogram recorded from the surface of nitrided AISI H13 samples: (a) as-received sample, (b) ground sample, (c) polished sample, and (d) lapped sample

Table 1 Nitrided surface roughness and lattice spacing, 2θ position, and effective case depth of gas-nitrided AISI H13 samples

Sample	R_a, μm before nitriding(a)	2θ, degree α-Fe (110)	Lattice spacing *d*, Å for α-Fe (110)	Effective case depth at 700 HV, μm
As-received	...	...	...	75
Ground	0.13 ± 0.035	43.80	2.06522	135
Polished	0.08 ± 0.015	43.70	2.06971	120
Lapped	0.04 ± 0.009	43.68	2.07061	85

(a) R_a values are given as average ± standard deviation

of free atomic nitrogen available to diffuse into the matrix due to more surface activation by grinding process. This observation is in line with relatively high nitride XRD peaks in the case of ground sample. Iron oxide (Fe_2O_3/Fe_3O_4) peaks as revealed in XRD measurement detected from the surface of roughened samples is an indication of oxidation due to partially oxidized rough surface prior to nitriding process.

3.2 Microscopic Observations in Diffusion Zone

The microstructures of the nitrided cross sections of as-received, ground, polished, and lapped sample surfaces observed under the optical and scanning electron microscopes are shown in Fig. 3(a) to (h). All microstructures consist of an

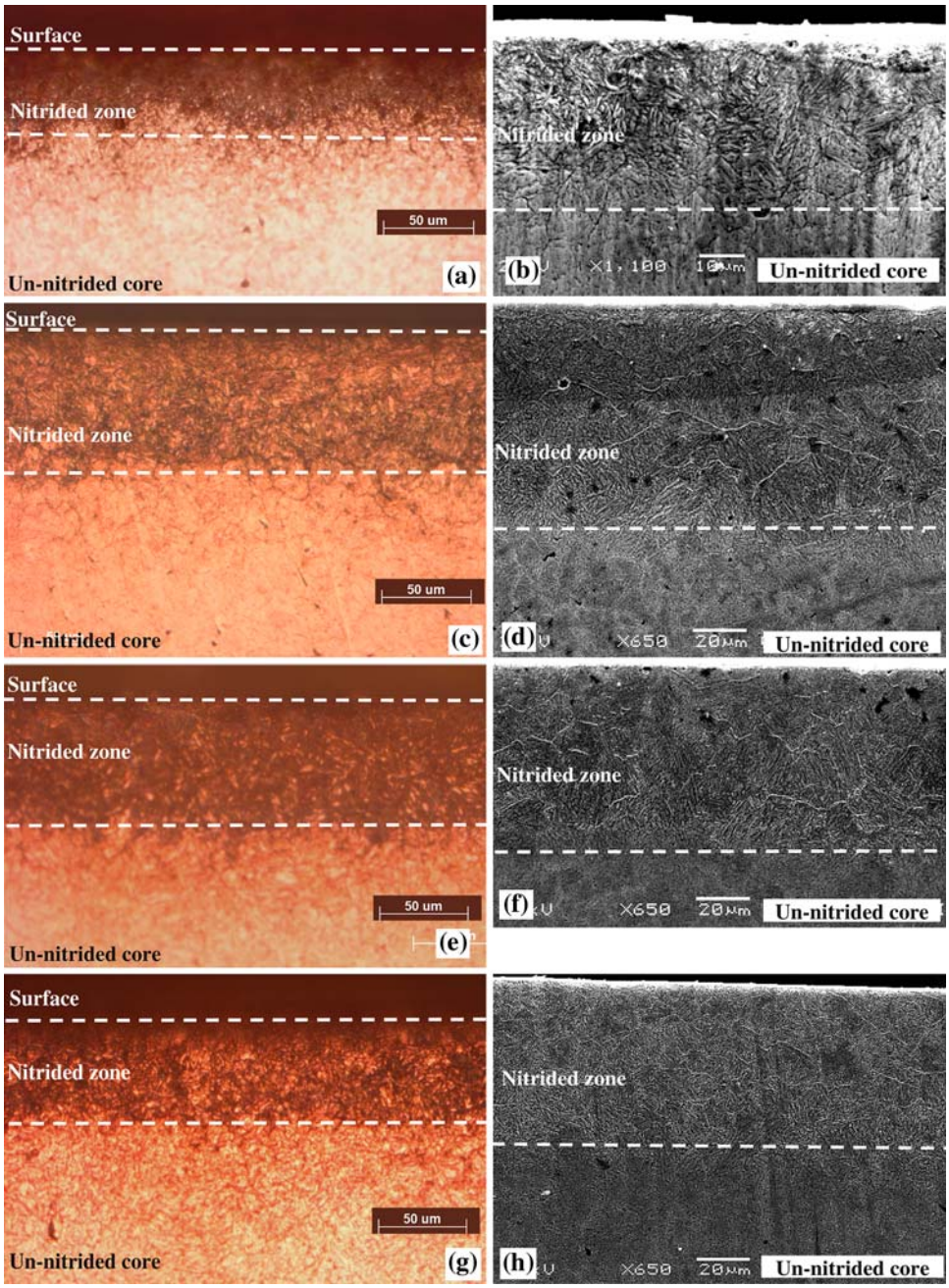

Fig. 3 Optical and scanning electron micrographs of nitrided cross sections: as-received sample (a, b); ground sample (c, d); polished sample (e, f), and lapped sample (g, h)

internal core of tempered martensite and a nitrided layer at the free surface. The nitrided layer consists of a diffusion zone with fine nitride precipitates (dark regions in the optical and lamellae structure in the SEM micrographs) and a compound layer at the surface. It is clearly visible from the microstructures that surface texture has significant implication on the thickness and uniformity of nitrided layer. The shallow and uneven nitrided layer in the case of as-received sample is due to the insufficient nitriding treatment, which greatly depends upon the ability of free atomic nitrogen to diffuse into iron matrix. If the surface is not properly textured via mechanical surface treatment, any expected superficial film or deposit, even of infinitesimally small thickness, can partially or completely prevent the access of active nitrogen to the surface and the availability for reaction of nitrogen that manages to get through the film can be insufficient (Ref 6). This, in turn, results in the insufficient quantity of submicroscopic nitrides that could precipitate during the nitriding cycle, as can be seen from SEM micrograph in Fig. 3(b). Unlike untreated sample surface, all the surfaces textured depict deep and uniform diffusion zones with some differences in depths. The diffusion zone increases with increase in initial surface roughness. Moreover, the ground sample resulted in deep diffusion zone followed by polished sample. Lapped sample with lowest surface roughness has the lowest depth of diffusion zone among the surface-textured samples. As indicated earlier, reduced lattice spacing with

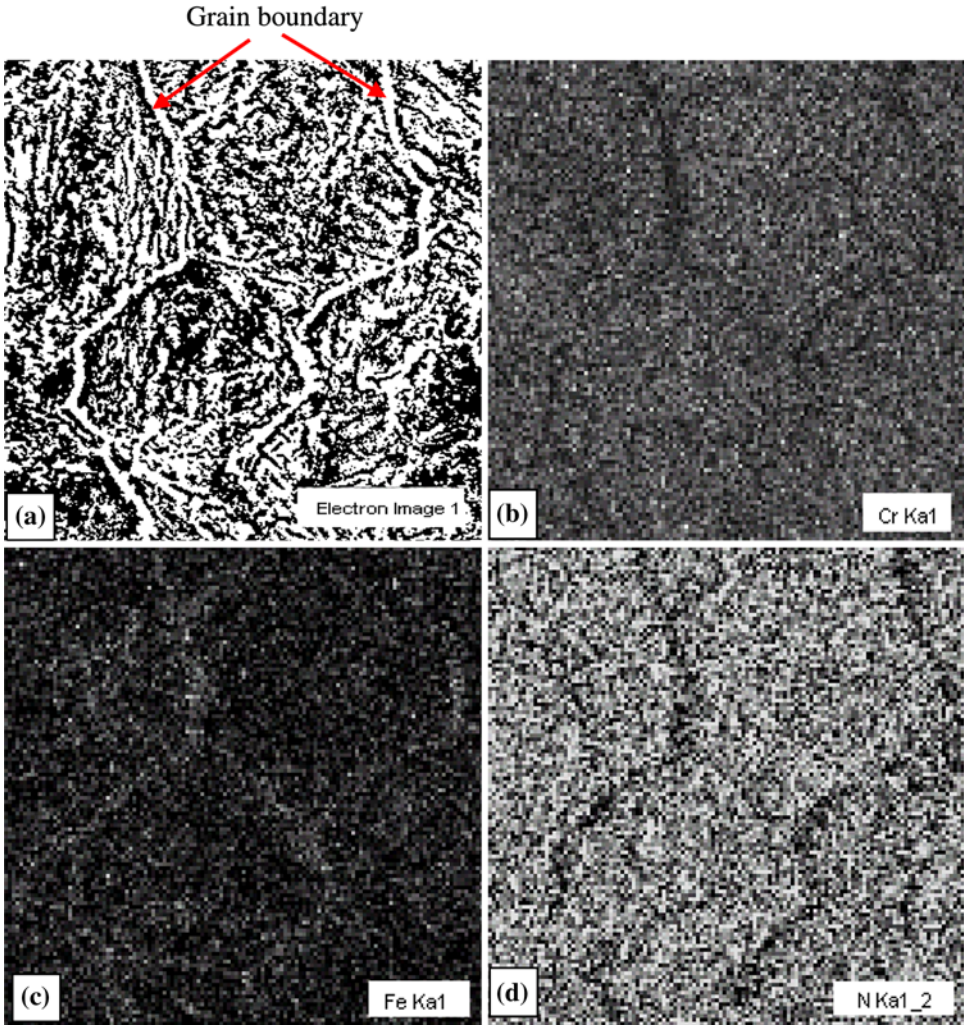

Fig. 4 EDS mapping result of diffusion zone of ground sample: (a) scanning electron image, (b) chromium content, (c) iron content, and (d) nitrogen content

increased roughness facilitates enhancement of nitrogen diffusion and hence, depth of diffusion zone increases with increasing surface roughness.

Examination of SEM micrographs reveals lamellae morphology in the diffusion zone of all samples. Surface-textured samples reveal sufficiently precipitated diffusion zone, which consisted of dense lamellae morphology. Such lamellae can be identified as Fe and nitrides of alloying elements, mainly CrN. The presence of CrN and ferrite (α-Fe) is also evident from XRD diffractogram of surface-textured samples with thin compound layers (Fig. 2). The peaks are likely to be detected from the uppermost region of diffusion zone beneath the compound layer as the Cu-K_α radiation probes up to only few microns. Cr is the main alloying element in AISI H13 steel (5.3%) which has relatively strong interaction with nitrogen during nitriding process. It was observed (Ref 3, 11) that submicroscopical coherent nitrides of Cr and other alloying elements like V, Mo, etc. developed during the initial stage of the nitriding process. However, extending nitriding process results in subsequent discontinuous coarsening, which leads to a lamellar microstructure as observed from SEM micrograph. This is also confirmed by EDS mapping of diffusion zone, which is observed over the diffusion zone as shown in Fig. 4. The enrichment of Cr and N_2 at the grain boundaries shows that grain boundary is the favorable diffusion path. Comparatively, fine lamellae structure can be observed near the surface region than near the un-nitrided core. This can be associated with higher nitrogen content in the near-surface zone as compared to the near-core zone.

3.3 Microscopic Observations in Compound Layer

The compound layer formed at the surface of as-received, ground, polished, and lapped samples is shown in Fig. 5. Unprepared sample has uneven and thick compound layer as compared to the surface-textured samples. The thick compound layer can strongly be associated with slow diffusion rate and nitrogen pressure at the surface. Among the surface-textured samples, ground sample has more uniform and slightly thicker (2.5-3 μm) compound layer as compared to polished (∼1.5 μm) and lapped (∼1 μm) samples. The thickness of compound layer for the samples is in line with the diffusion zone thickness, which reduces with decreasing surface roughness. This can be associated with high XRD counts of iron nitrides for ground sample, particularly mixed phase peak of ε-Fe_3N(002) + γ′-Fe_4N(111) as observed from XRD diffractogram.

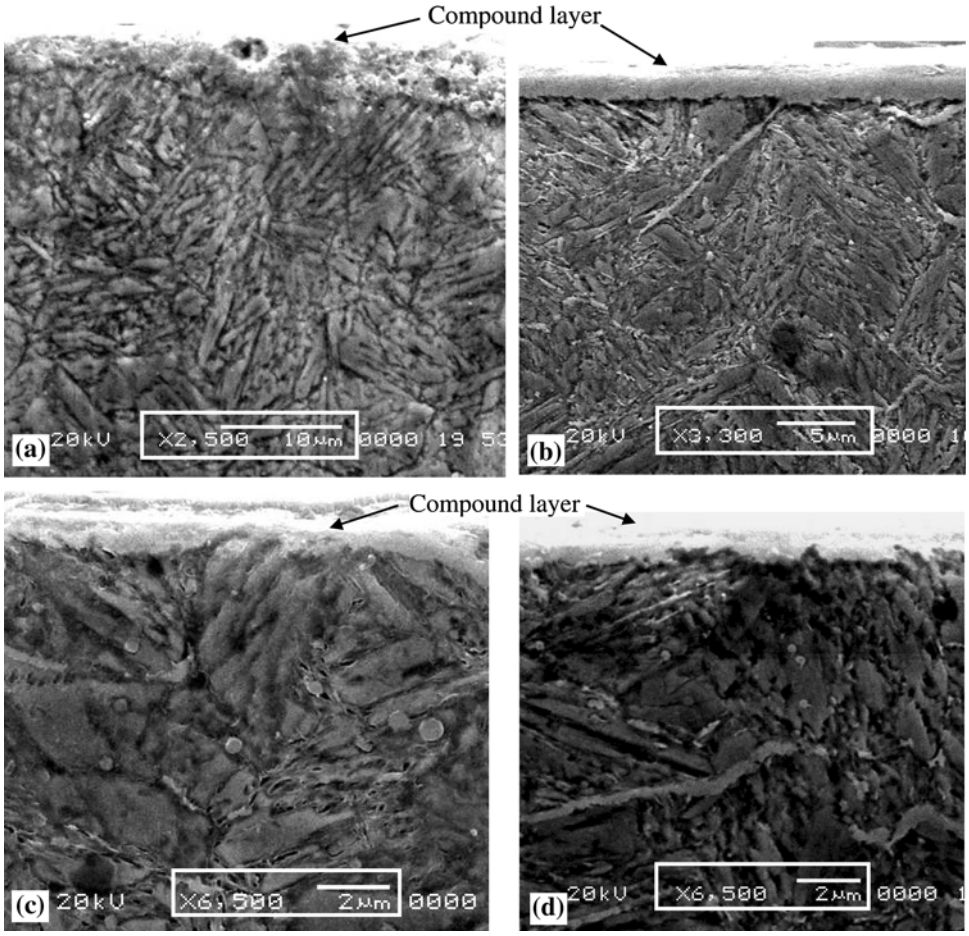

Fig. 5 Magnified SEM images of compound layer developed after controlled gas nitriding at the surface of as-received specimen (a); ground specimen (b); polished specimen (c); and lapped specimen (d)

The actual variation of K_n as shown in Fig. 1(b) indicates that the compound layer should form at the surface with high concentration of ε-phase in line with the SEM and XRD results. The critical nitriding potential values and hence the nitrogen activities above which the iron nitrides in the compound layer (γ'-Fe_4N and ε-Fe_3N) develop can be identified. The Lehrer's equilibrium diagram (Ref 10), which illustrates the relationship between nitriding potential (K_n), the nitriding temperature, and the α, γ', and ε phases in equilibrium, can be used to observe the effect of nitriding potential on the formation of the ε or γ' phases in the surface. It is assumed that the shifts in the Lehrer diagram caused by alloying elements are not large and can be used for H13 steel (Ref 4). It is evident from Lehrer equilibrium diagram that the γ'-Fe_4N phase of compound layer begins to form when K_n exceeds the upper limit of N concentration in the α zone (diffusion zone). Further increase of K_n causes the formation of the ε phase in the surface region of the steel. The variation of nitrogen activity at the surface of the sample is shown in Fig. 6, which reveals that the K_n values during the nitriding cycle (Fig. 1b) allows the formation of ε phase in the surface region of un-nitrided sample based on the upper and lower limits of the γ' phase field as shown in Fig. 6. The upper and lower limits of the γ' phase field are based on the report by Kooi et al. (Ref 12), who developed the relationship between nitriding potential and temperature for the α-γ' and γ'-ε phase boundaries for the activities of nitrogen.

3.4 Comparison of Hardness-Depth Profiles and Case Depth of Nitride Layer

Figure 7 presents the variations in microhardness of nitrided layer as a function of the case depth for untreated and surface-treated samples, which were gas nitrided under the controlled nitriding potential. Each point represents the average value of five indentations in the curves. The average maximum hardness of the as-received specimen was observed to be in the range of about 1050 HV maintained up to a distance of ~20 µm, which then decays to core hardness of about 650 HV monotonically with increasing distance from the surface. The average maximum hardness is quite low in magnitude in comparison with the surface-roughened samples. The reduced hardening effect is due to insufficient precipitation as a result of inadequate surface preparation. The average maximum hardness of surface-textured samples is about 1280 HV, which is maintained for a depth about 40 µm below the surface. Among the surface-treated samples, the maximum hardness is slightly higher for polished sample up to a depth of 20 µm below the surface. Important differences can be observed among the hardness profiles of surface-treated samples concerning the steepness of the curve and effective case depth, which is an indication of load-bearing capacity of the nitrided case. The hardness curve for lapped sample is steeper than the ground and polished samples. Polished sample

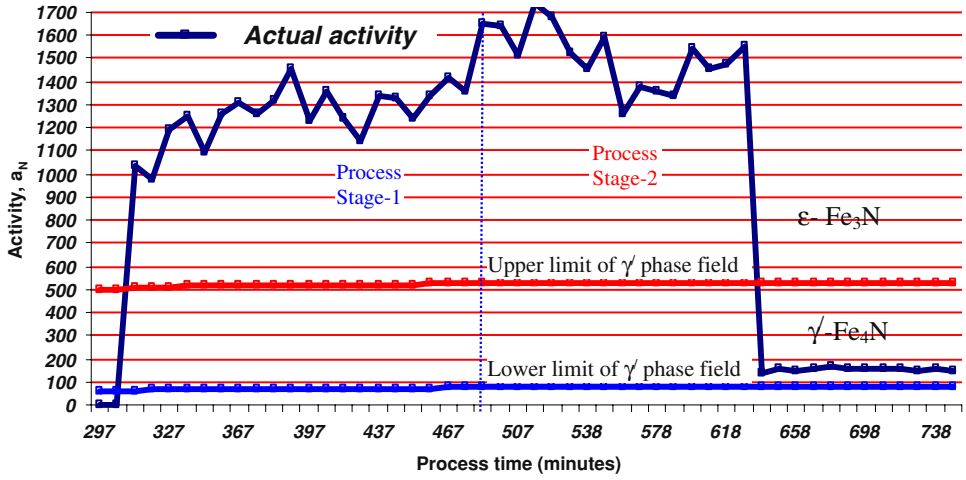

Fig. 6 Variation of nitriding activity at the surface of the sample in the nitriding stages. The upper and lower limits of γ′ phase field for un-nitrided H13 sample are also shown

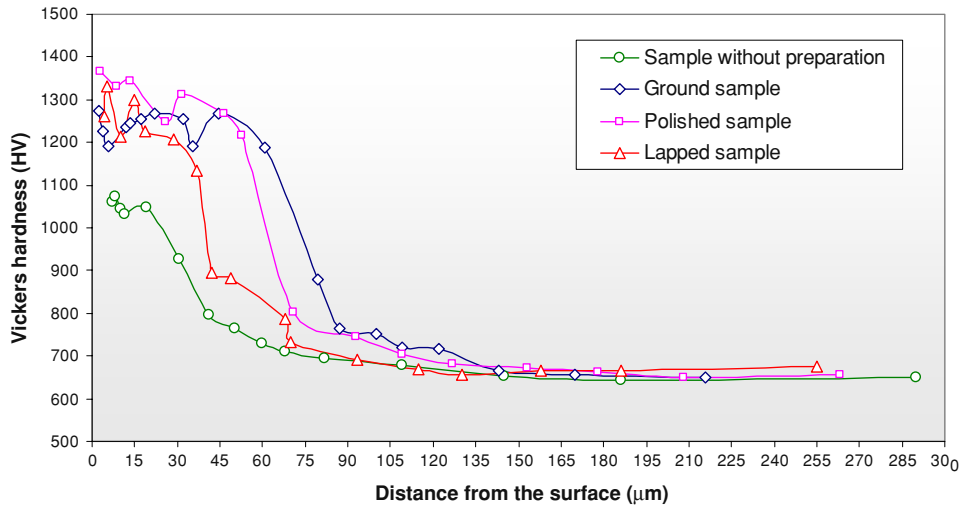

Fig. 7 Vickers hardness-depth profiles of nitrided cross section for as-received, ground, polished, and lapped samples

showed a steeper curve with reduced hardening effect near the core region as compared to ground sample. The effective case depth, which is defined as the depth where the hardness was approximately 700 HV (based on the criterion set forth by ASM for H13 steel), is given in Table 1. The effective case depth increases with surface roughness and it attains the highest value for ground sample followed by polished sample. This finding is in agreement with the previous results in which it was shown that diffusion zone increases with increased surface roughness. It should be noted that near the surface where the nitrogen content is maximum, the driving force for precipitation of nitrides is the maximum, causing more abundant nucleation of fine lamellae structure as observed in SEM micrographs of the nitrided samples' cross section. Therefore, the decay of hardness across the nitrided layer cross section can strongly be related with the decay of nitrogen concentration from surface to the core.

4. Conclusions

The influence of mechanical pretreatment (surface texture) in terms of surface roughness on nitriding kinetics of AISI H13 tool steel during controlled gas nitriding was studied. It is found that the surface texturing by surface roughening prior to nitriding enhances significantly the nitriding kinetics and is expected to increase wear resistance of H13 steel used for aluminum extrusion die while resulting in its increased service life. Following specific conclusions can be drawn from the results obtained:

1. The XRD analysis confirmed that the compound layer consists of iron nitrides mainly ε-Fe_3N phase and small fractions of γ′-Fe_4N phase, which was expected from the values of in-process varying nitriding potential during

gas-nitriding cycle. Ground sample has more uniform and slightly thicker (2.5-3 μm) compound layer as compared to polished (∼1.5 μm) and lapped (∼1 μm) samples.

2. Unprepared sample (without surface preparation) results in uneven and shallow nitride case depth. In addition, hardness reduces due to insufficient nitride precipitation during nitriding.
3. Surface-textured samples revealed sufficiently precipitated diffusion zone, which consists of dense lamellae morphology is identified as Fe and CrN using EDS mapping.
4. Ground sample with high surface roughness exhibits deeper diffusion zone and effective case depth as compared to polished and lapped samples. This can be associated with the reduction in lattice spacing of α-Fe. The reduction in lattice spacing suggests comparatively large number of free atomic nitrogen, which is available for diffusion and induction of high compressive stress at the surface.
5. The average maximum hardness of the untreated specimen is found to be about 1050 HV (maintained up to a distance of ∼20 μm) which increases to about 1280 HV (maintained up to 40 μm) in the case of surface-textured samples. Ground sample results in less steep and gradual decay of hardness curve followed by polished and lapped samples.

Acknowledgments

The authors acknowledge the support of King Fahd University of Petroleum and Minerals, Dhahran, Saudi Arabia for the funded project, Project # SB080002 and ALUPCO, Saudi Arabia for this work.

References

1. E.J. Mittemeijer and J.T. Slycke, Chemical Potentials and Activities of Nitrogen and Carbon Imposed by Gaseous Nitriding and Carburizing Atmospheres, *Surf. Eng.*, 1996, **12**(2), p 152–162
2. T. Liapina, "Phase Transformations in Interstitial Fe-N Alloys," PhD Thesis, Institut fur Metallkunde der universitat Stuttgart, Max-Planck-Institut fur Metallforschung Stuttgart, 2005
3. N.V. Díaz, "Nitriding of Iron-Based Alloys; Residual Stresses and Internal Strain Fields," PhD Thesis, Max-Planck-Institut fur Metallforschung Stuttgart, 2007
4. W.K. Liliental, A. Czelusniak, C.D. Morawski, and G.J. Tymowski, Getting More Life Out of the Aluminum Extrusion Die by Controlled Gas Nitriding, File: T-Tech\TP\PPR\TPAI001.doc, Nitrex Metal Inc., 1999
5. H. Sueyoshi, K. Hamaishi, Y. Nakamura, and J. Kiyofuji, Effect of Mechanical Pre-treatment on Gas Nitriding Behavior in Austenitic Stainless Steels, *Mater. Trans. JIM*, 1996, **37**(2), p 150–156
6. A. Czelusniak, W.K. Liliental, and G. Tymowski, Influence of Die Handling Operations on Performance of Nitrided Aluminum Extrusion Dies, File: T\TP\PPR\ET SE001.doc, Nitrex Metal Inc., 1997
7. D.H. Bei, J. Lu, J.F. Gu, K. Lu, and J.S. Pan, Effects of Surface Nanocrystallization Pre-Treatment on Gas Nitriding Behavior of Mild Steel, *Trans. Mater. Heat Treat.*, 2002, **23**(1), p 19–24
8. G. Wroblewski and K. Skalski, Properties of Surface Layer Generated by New Combined Process of Burnishing and Nitriding, *Surf. Eng.*, 2006, **22**(2), p 138–146
9. J. Baranowska, K. Szczecinski, and M. Wysiecki, Increasing of Gas Nitriding Kinetics via Surface Pre-Treatment, *J. Surf. Coat. Technol.*, 2002, **151–152**, p 534–539
10. Aerospace Material Specification for 'Automated Gaseous Nitriding Controlled by Nitriding Potential' (2579/10A), June 2006, http://frontiervalve.com/brochures/amsSpec.pdf
11. R.E. Schacheral, "Growth Kinetics and Microstructure of Gaseous Nitrided Iron Chromium Alloys," PhD Thesis, Institut fur Metallkunde der universitat Stuttgart, Max-Planck-Institut fur Metallforschung Stuttgart, 2004
12. B.J. Kooi, M.A.J. Somers, and E.J. Mittemeijer, An Evaluation of the Fe-N Phase Diagram Considering Long-Range Order of N Atoms in γ'-Fe_4N_{1-x} and ε-Fe_2N_{1-z}, *Metall. Mater. Trans. A*, 1996, **27**, p 1063–1071